

Diffusion of Two-Dimensional Particles on an Air Table

Luc Oger,¹ Chrystèle Annic,¹ Daniel Bideau,¹ Rongqing Dai,² and Stuart B. Savage²

Received September 19, 1994; final July 14, 1995

Rapid granular flow is diffusive in character. This diffusive nature is important in the generation of constitutive properties such as effective shear and bulk viscosities, effective conductivity of particle fluctuation energy, and self-diffusion coefficients. Experiments were performed in a large air-table apparatus that can sustain up to a few thousand small, light disks just above a horizontal porous plane. Experiments on 2D diffusion processes were performed using this apparatus. Measurements of self-diffusion coefficients and granular temperature in systems having different areal concentrations are in good agreement with predictions based on the kinetic theory and on numerical simulations.

KEY WORDS: Diffusion process; kinetic theory; image analysis; packing fraction.

1. INTRODUCTION

Diffusion has a strong effect on important processes in rapid granular flow in like-particle mixing and size and density segregation. Nevertheless, relatively few studies have focused on the prediction of diffusion coefficients in flow of dense granular systems. In the present paper, we present both experimental (using an air table) and numerical determinations of the self-diffusion coefficient for disklike particles and compare the results with predictions based on the kinetic theory. First, we describe a two-dimensional (2D) experiment designed to study the granular temperature and show how to determine the diffusion coefficient with new image-processing

¹ Groupe Matière Condensée et Matériaux, URA CNRS 804, Université de Rennes I, 35042 Rennes Cedex, France.

² Department of Civil Engineering and Applied Mechanics, McGill University, Montréal (QC) H3A 2K6, Canada.

techniques. Second, we develop the kinetic theory for uniform-sized disks and show that our experimental results can be understood in terms of a balance between the dissipation of inelastic, rough disks and the energy input from the random turbulent fluctuations from the air table. Third, we describe the results of computer simulations based on a hard-disk model and show how to calculate velocity autocorrelation functions to determine diffusion coefficients. Finally, we compare the results of experiments, kinetic-theory calculations, and computer simulations.

2. EXPERIMENTAL APPARATUS AND INSTRUMENTATION

We have designed and constructed a large air table in order to study the statistics of some two-dimensional systems.⁽¹⁾ A vertical wind tunnel provides a homogeneous air flux through a horizontal porous plate. Air passing through the pores supports small disks which constitute a more-or-less-dense, 2D particle system. The porous surface comprises a horizontal porous plate made of sintered bronze, 0.5 cm thick and 50 cm by 50 cm. The disks are styrene (density 1.18 g/cm³), 1 mm thickness and 8 mm diameter. A truncated Plexiglas pyramid-shaped hood of base 50 × 50 cm² and height 48 cm suspended 3 cm above the air table prevents the initial loss of pressure close to the boundaries of the table and thus allows uniform performance.

The disks experience what we might call 'hard-core interactions' (no overlapping or deformation between them) and eventually weak hydrodynamic interactions.⁽²⁾ Heterogeneities in air pressure and velocity at a small spatial scale are unavoidable because of the porous plate (pore size is around 40 μm): these heterogeneities and the lack of parallelism between the disks and the sintered plate cause chaotic motion of the suspended disks.

2.1. Granular Temperature Measurements

The system is dissipative because the blowing apparatus is a reservoir that ensures a steady state (not an equilibrium one) in which the energy lost in collisions is balanced by the energy gained by the system by interacting with the air flow. Experiments suggest that the disks are never perfectly horizontal after a collision. These deviations from the horizontal may be caused by geometrical defects of the disks or because collisions are never frontal. After collisions, particles are subject to forces resulting from the presence of air under them. Acceleration appears to be uniform (Fig. 1). In the short term, all the particles accelerated in approximately the same manner. As time t after the collision increases, the probability that a first

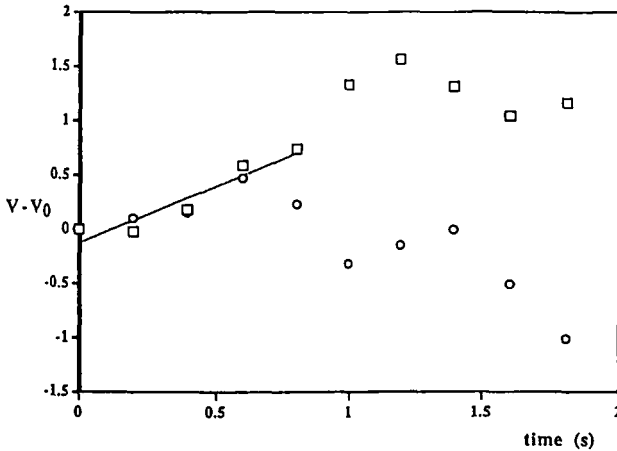


Fig. 1. Increase of velocity versus time for different packing fractions of disklike particles on the air table. V is the instantaneous velocity calculated between two consecutive time steps, V_0 is the initial velocity obtained just after the collision, $\nu = 0.007$ for the square, and $\nu = 0.08$ for the circle.

particle moves freely without experiencing a new collision decreases proportionally as the packing fraction (areal fraction occupied by the disk on the plate) increases. The mean free path is inversely proportional to the density number of particles and hence the packing fraction. Thus only the slow-moving particles have long enough intervals between collisions to be included in average calculations. This is why the discontinuity in the variation of $V - V_0$ versus time appears at $t = 0.8$ sec for a packing fraction $\nu = 0.08$ and at $t = 1.2$ sec for a packing fraction $\nu = 0.007$.

During a given time step, the measurement of the local displacements can be used to generate a velocity distribution function. This distribution approximates a Maxwellian and thus permits the calculation of the temperature. In the case of gas this would be given by

$$T = \frac{m}{2k} \langle V^2 \rangle \quad (1)$$

where k is Boltzmann's constant and m is the mass of the grain. In the case of granular media⁽³⁾ the definition of granular temperature omits k/m , and the granular temperature T_g becomes proportional to the mean square of the velocity fluctuations⁽³⁾:

$$T_g = \frac{1}{2} \langle V^2 \rangle \quad (2)$$

To better understand the granular temperature, we have performed three kinds of measurements:

(a) First for one given air flow, we have varied the number of particles on the table in order to vary the packing fraction from 0.05 to 0.22.

(b) Air flow was changed to a higher value while packing fraction was varied over the same range as in (a).

(c) For the same air flow as in (a), and for a fixed packing fraction of 0.025, particle diameter was varied.

2.1.1. Measurements at Standard Air Flux. The air flow passing through the porous plate comes from two electric fans with adjustable electric voltage inputs.⁽¹⁾ The major part of our granular temperature experiments were performed with a standard air flux which corresponds to an electric voltage of 150 V. For a chosen packing fraction, we placed a given amount of disks on the table and began the experiment. All the particle displacements were recorded with a video camera. By looking at a series of consecutive video images (each separated by 1/25 sec), we can easily calculate the velocity of each disk corresponding to a given time step. For each time step, all the local velocities are measured and recorded except the velocity of particles which are involved in collisions (between two particles or with the boundaries of the table). For the low packing fraction, several independent velocity measurements are performed to obtain a good statistical averaging (Fig. 2). Table I summarizes results obtained for different values of packing fraction up to 0.22, the largest packing fraction for which it is still possible to measure the velocity distribution function without eliminating too many of the velocity values

Table I. Granular Temperature T_g and the Packing Fraction ν of Particles for Air-Table Experiments with Air Flow Passing Through the Porous Plate of the Table

ν	Granular temperature T_g	
	Normal air flow	Increased air flow
0.0056	19.43	19.43
0.01	17.81	20.65
0.025	13.15	19.3
0.056	11.71	13.3
0.11	7.56	11.80
0.16	6.72	—
0.22	6.41	8.73

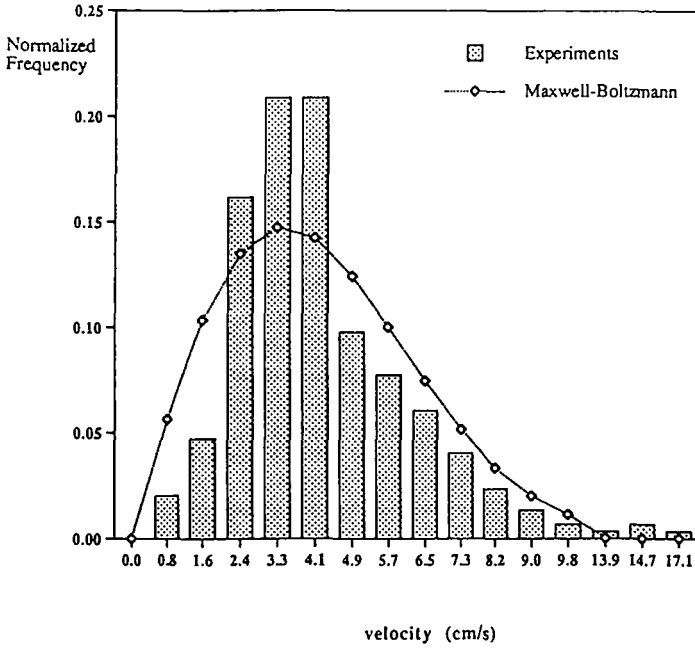


Fig. 2. Velocity distribution function obtained for a packing fraction of 0.11. This distribution is compared to a Maxwell-Boltzmann distribution.

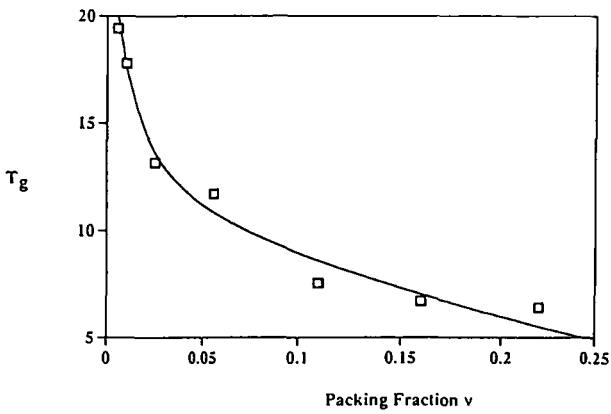


Fig. 3. Granular temperature T_g versus packing fraction.

Table II. Normalized Granular Temperature Showing Relatively Small Temperature Variations

σ (cm)	Temperature T_g	T_g/area
0.6	5.27	18.64
0.8	13.19	26.25
1.0	18.41	23.45
2.0	118.82	37.82

(because of the number of collisions which occur during a given time step). Temperature varies logarithmically with the packing fraction ν ($R^2 \sim 0.99$) (Fig. 3). An extrapolation of this curve for the packing fractions ranging from 0.25 to 0.77 is used for the next measurements discussed in Section 2.2.

2.1.2. Measurements at Higher Air Flux. We have repeated the experiments with increased air flux. This flux increases the height of the particles above the air table^(1,4) so that their mean velocities V_0 increase (Table I). As in the previous case, the temperature is found to vary logarithmically with the packing fraction with a new factor which depends on air pressure.

2.1.3. Measurements for Different Disk Sizes. The preceding section shows that granular temperature is dependent on the height of the particle above the porous plate. We wish to obtain a mass-weighted granular temperature as in Eq. (1). Because disks of differing size have the same thickness and mass density, disk weight is proportional to disk area. A normalized granular temperature (T_g divided by area) for four disk sizes (0.6, 0.8, 1.0, and 2.0 cm) is seen to be approximately constant as shown in Table II.

To summarize, granular temperature varies with packing fraction up to $\nu = 0.22$ and we infer that this temperature will decrease to zero as packing fraction approaches the densest possible 2D packing [$\pi/(2\sqrt{3}) \sim 0.906$].

2.2. Diffusion Measurements

An accurate analysis of the diffusion process on the air table is only possible if we analyze the diffusion paths for a large number of particles. To perform these measurements, we have developed an automatic, real-time

image-processing system. The accurate location of one marked particle is very important. For this reason, we have used a camera with a digitizer board having a resolution of 752×468 pixels and a video frame which covers the complete air table ($50 \times 50 \text{ cm}^2$). The marked particle has a diameter of 8 mm and corresponds to about 8 pixels, which is large enough to calculate and record the position of the center of this particle.

Storing a full 2D image on a computer is not only unnecessary, but it consumes such a large amount of hard disk space that it would be impossible to store a continuous movie of the displacement of the marked particle for the desired times. We have solved this problem by creating an image-analysis loop so that the only outputs are the coordinates of the marked particle center. This loop is composed of the following simple image-processing functions:

1. Grabbing the image.
2. Making a threshold of the gray-level image to create a binary image.
3. Locating the particle and calculating the coordinates of its center.
4. Storing this result on a file and going back to the beginning of this loop. The minimal duration of this loop is about 2 sec.

For this experiment, the particles have to stay in a confined area. In order to study the diffusion process of these particles we have to define some simple rules to improve the quality of our results.

1. The trajectory of only one marked particle is recorded at a given time.
2. The marked particle was placed near the center of the air table and the air flow was activated before the beginning of the run.
3. Only the initial part of the trajectory of the particle is recorded; if the particle touches the boundaries of the air table, this experiment ceases.

For each packing fraction, we recorded 200 trajectories to obtain statistically accurate mean-square particle displacements versus time. Because of the large fluctuations of mean-square displacement values, only the common part of the 200 results is used for the fit calculation. The linear fit of the mean-square displacement versus the time yields the value of the self-diffusion coefficient D :

$$\langle \Delta R^2 \rangle = 4Dt \quad (3)$$

The measurements of the mean square displacement are performed only for packing fractions between 0.25 and 0.77. For lower packing fractions, the time for the marked particle to touch the wall is so short that the numbers of consecutive coordinates are too few to estimate an accurate self-diffusion coefficient. Table III gives a full set of our results. A plot of the variation of the self-diffusion coefficient versus the packing fraction (Fig. 4) shows two regions of the curve. At packing fractions from 0 to about 0.7, the self-diffusion coefficient decreases linearly with the packing fraction when results are plotted using a log scale. But a high packing fractions near 0.74, the slope of the self-diffusion coefficient changes drastically. This change corresponds to the transition between a real 2D disordered packing of disks and the appearance of local ordering among the particles⁽²⁾ as predicted by Bideau *et al.*⁽⁵⁾ The difference between our result (0.74) and the result (0.82) given by Hinch and Lemaitre⁽²⁾ is due solely to the way of calculating the packing fraction. Hinch and Lemaitre⁽²⁾ define an effective diameter larger than the geometrical one (by 8%) to allow for short-range repulsive potential between the disks. When this correction was made, our results agree with these of Hinch and Lemaitre.⁽²⁾

We require a global theory to correlate measurements of granular temperature at low packing fractions and the self-diffusion coefficients at high

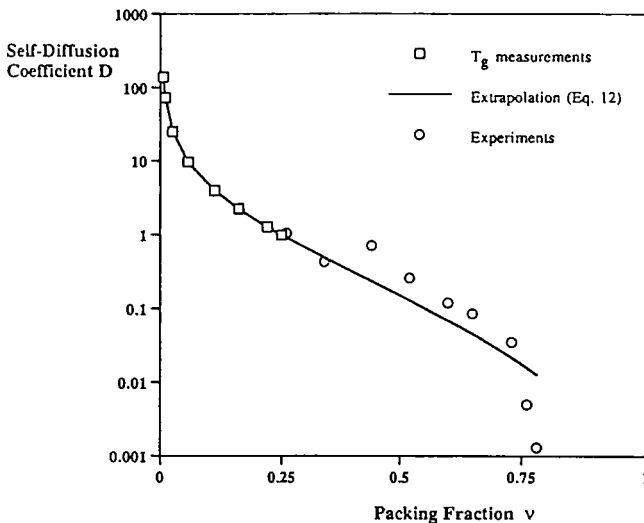


Fig. 4. Self-diffusion coefficient versus the packing fraction. Experimental results of D are for packing fractions between 0.25 and 0.77. The curve is an extrapolation of the granular temperature using the kinetic theory.

Table III. Self-Diffusion Coefficient for 2D Random Particle Motion Versus the Packing Fraction

Packing fraction ν	Self-diffusion coefficient D
0.26	1.04×10^0
0.34	4.3×10^{-1}
0.44	7.1×10^{-1}
0.52	2.6×10^{-1}
0.60	1.2×10^{-1}
0.65	8.5×10^{-2}
0.73	3.5×10^{-2}
0.76	5.0×10^{-3}
0.78	1.3×10^{-3}

packing fractions. In the next section, we describe a kinetic-theory diffusion coefficient that can be applied to the 2D air table experiment.

3. KINETIC THEORY

Kinetic theories of granular flows have been developed following the approaches used in the kinetic theories of dense fluids and liquids. They incorporate energy dissipation owing to inelasticity and surface roughness. Both the granular temperature and the normalized velocity autocorrelation function $a_v(t)$ can be determined by means of such kinetic theory approaches. Analyses of T_g and $a_v(t)$ for granular flows of disklike particles are now described.

Following the work of Einstein⁽⁶⁾ on Brownian motion and applying it to the 2D random motion of a particle, one finds that the self-diffusion coefficient D is given by Eq. (3). Further, the mean square of the particle displacement due to random walk can be expressed as

$$\langle \Delta R^2 \rangle = 2t \int_0^\infty \langle \mathbf{C}(0) \cdot \mathbf{C}(\tau) \rangle dt \quad (4)$$

where \mathbf{C} is the peculiar velocity and $\langle \mathbf{C}(0) \cdot \mathbf{C}(\tau) \rangle$ is the velocity autocorrelation function. Note that \mathbf{C} is the difference between the instantaneous particle velocity and the local mean velocity, $\mathbf{C} = \mathbf{c} - \mathbf{u}$. Hence, the self-diffusion coefficient may be expressed as

$$D = \frac{1}{2} \int_0^\infty \langle \mathbf{C}(0) \cdot \mathbf{C}(\tau) \rangle d\tau \quad (5)$$

The integral of Eq. (5) is evaluated by kinetic theory methods. Considering that one-half of the initial value of velocity autocorrelation function is the granular temperature of the system, we may write

$$D = T_g \int_0^{\infty} a_v(t) dt \quad (6)$$

where $a_v(t)$ is the normalized velocity autocorrelation function,

$$a_v(t) = \frac{\langle \mathbf{C}(0) \cdot \mathbf{C}(t) \rangle}{\langle \mathbf{C}(0) \cdot \mathbf{C}(0) \rangle} \quad (7)$$

Following the usual practice, we assume the velocity autocorrelation function to be an exponential decaying function of time,

$$a_v(t) = \exp(-\beta t) \quad (8)$$

where β is a constant that can be determined from (7) and (8) as

$$\beta = - \left. \frac{da_v(t)}{dt} \right|_{t=0} = - \lim_{\Delta t \rightarrow 0} \frac{\langle \mathbf{C} \cdot \Delta \mathbf{C} \rangle}{2T \Delta t} \quad (9)$$

and where $\Delta \mathbf{C} = \mathbf{C}(t + \Delta t) - \mathbf{C}(t)$.

By applying the kinetic theory of granular flows to analyze the collisional processes of identical, smooth, inelastic disks, one finally finds that

$$\beta = \frac{8\nu g_0(\nu)}{\sigma} \left(\frac{T_g}{\pi} \right)^{1/2} \quad (10)$$

where g_0 is the radial distribution function at contact (deduced from ref. 7)

$$g_0(\nu) = \frac{16 - 7\nu}{16(1 - \nu)^2} \quad (11)$$

and σ is the particle diameter, ν the solid fraction, and T_g the granular temperature.

Substituting Eqs. (10) and (8) into Eq. (6), we obtain the final expression for the self-diffusion coefficient,

$$D = \frac{\sigma(\pi T_g)^{1/2}}{8\nu g_0(\nu)} \quad (12)$$

Thus, knowing the granular temperature at a given solid fraction and using Eq. (12), we can determine the self-diffusion coefficient D . Figure 4 gives D calculated from Eq. (12), where T_g is measured in air-table

experiments. In Section 2 we assumed that the granular temperature curve for low packing fractions could be extrapolated to the high packing fractions. The curve of the self-diffusion coefficient in Fig. 4 shows this extrapolation to $\nu=0.80$. This curve gives also a good fit to the results of the direct measurements of the self-diffusion coefficient. This comparison will be given in Section 5 after we describe the numerical simulations of these experiments.

4. COMPUTER SIMULATIONS

The computer simulations are performed using a molecular dynamics model. The particle-interaction model used in our simulation is the so-called hard-particle model which assumes instantaneous collisions. In the air table when the fluctuating particles have reached an equilibrium state, there is a balance between the collisional energy dissipation in the particles and the energy input to the particles from the fluidizing air. To model their behavior in a simple way, we have merely taken the particles to be perfectly elastic and given the mass of particles initial velocities appropriate to a chosen granular temperature.⁽⁷⁻⁹⁾

In the simulations, the particles are initially placed in a square computational box and are given random velocity fluctuations about a mean shear flow velocity. Initially, the particles are placed in a regular array according to the number of particles and the packing fraction needed. At the first step, all lengths are nondimensionalized by H , the dimension of the computational box, and velocities are nondimensionalized by U , a characteristic velocity associated with the shear flow at the boundaries. To eliminate the difficulties associated with obtaining the desired granular temperature, we first perform a random choice of the initial local velocities, then we calculate the corresponding granular temperature as previously defined. After this calculation, we normalize our granular temperature to the unit by dividing the previous velocity values by the calculated square of the temperature. During our numerical simulations, as we have no loss of energy, we did not need to check the fluctuations of this granular temperature; at the end of the run we calculate the energy and it remains constant and equal to the unit according to the numerical error.

According to the positions and the velocities of each of the disklike particles, we calculate the shortest time Δt before the next collision between particles, increase the time by this amount, implement the collision, again calculate the next shortest time step, and so on. Simple periodic boundary conditions were applied on all the walls of the computational box to effectively increase the size of the computational region. When a particle crosses a boundary, it is introduced at the corresponding position in the wall of the opposite side of the 2D box.

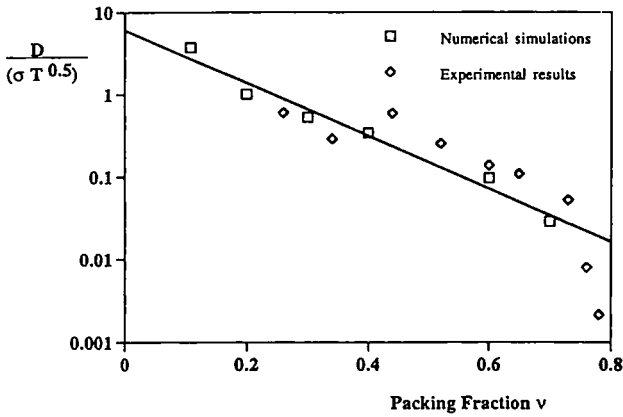


Fig. 5. Dimensionless self-diffusion coefficient $D/(\sigma\sqrt{T_g})$ versus packing fractions from two kinds of studies: (a) experimental studies with packing fractions between 0.25 and 0.77; (b) numerical simulations of hard disks with packing fractions between 0.1 and 0.7.

As the initial parameters are the X, Y coordinates and the U_x, U_y velocities in a regular lattice, we need to perform a large number of collisions before we can be sure that we have a homogeneous, random, disordered, moving-disk arrangement. We performed 50,000 collisions before determining the granular temperature and the self-diffusion coefficient.

In order to calculate the self-diffusion coefficient, we must integrate the autocorrelation function with respect to time. This operation has been done by calculating the autocorrelation function after each 100 collisions and by accumulating the results. The simulations were performed for up to 1,000,000 collisions to obtain accurate values of the autocorrelation function.

Table IV. Normalized Self-Diffusion Coefficient $D/(\sigma\sqrt{T_g})$ for 2D Random Particle Motion Versus the Packing Fraction

ν	$D/(\sigma\sqrt{T_g})$
0.11	3.730
0.20	1.010
0.30	0.530
0.40	0.343
0.60	0.097
0.70	0.029

In our simulations, we have kept the size of the box and the granular temperature (one-half of the mean square of particle velocity fluctuation) constant, and increased the number of particles inside the box to have a packing fraction varying from 0.11 to 0.70. The simulations were performed for times sufficient to have an autocorrelation function close to zero. Owing to the dimensionless input parameters (the velocity is initially divided by the square root of temperature, the size of the box is normalized by disk diameter), the results have been obtained as a dimensionless value of the self-diffusion coefficient $D/(\sigma \sqrt{T_g})$. The numerical results are presented in Table IV and Fig. 5. In this figure, the decrease of the self-diffusion coefficient with the packing fraction is similar to that of previously mentioned experiments. We shall discuss this comparison in more detail in the next section.

5. COMPARISON AND DISCUSSION OF RESULTS

The principal conclusion of our three kinds of studies is the good correlation between the experimental and theoretical results. Although the detailed mechanics in the physical experiments differs from that in the numerical simulation, the correspondence of the normalized self-diffusion coefficients suggests surprising and interesting similarities. In the air-table experiments, the disklike particles moved inside a box with hard boundaries which confines the particles inside it, but in the numerical simulations we apply periodic boundary conditions to the particle motions. The real particles move on the air table as a result of energy coming from the air flow. In the molecular dynamics simulations, we started with an initial energy for the set of particles. Since the restitution coefficient in the simulation is equal to 1, the total 'mean' energy remains constant during the run. In the experiments we can infer that the energy input from the air flow under the particles is equal to the loss of energy due to the collisions between particles. Thus we average over long times to determine the mean square velocity fluctuations. The process is stationary and we can determine the growth of the mean square displacement with time to calculate the diffusion coefficients.

By using a dimensionless value for the self-diffusion coefficient $D/(\sigma \sqrt{T_g})$, Eq. (12) becomes a simple function of the packing fraction according to the radial distribution function at contact $g_0(v)$. The good agreement between the kinetic theory, the experiments, and the numerical simulations gives us important information about the mean phenomena which govern the displacement of the particles on the air table. These displacements were found to occur randomly over the whole air table, indicating homogeneity in the air flow and horizontal alignment of the table.

The mean free path between particles and the self-diffusion coefficient are related to one another such that the self-diffusion coefficient decreases with the packing fraction. We also conclude that (at a given air flow velocity) the granular temperature decreases continuously with increase in packing fraction until ordering of the disks occurs ($\nu \cong 0.77$).^(4,5) Even if it was not possible to measure this granular temperature for the high value of the packing fraction, the experimental and numerical variations (Fig. 5) of the dimensionless self-diffusion coefficient with packing fraction permit us to conclude that the extrapolation of this temperature works well. This extrapolation is, however, limited by the appearance of particle ordering.^(4,5) Above a packing fraction about 0.74, the correlation between experimental and numerical results and kinetic-theory predictions is poor.

It would be desirable to have, for the same packing fraction, the granular temperature and the self-diffusion coefficient to avoid misleading interpretations about the mean phenomena which occur in our air-table experiments. For that, we need a very fast video camera system (up to 1000 images per second) to record all the local displacements and hence to calculate all the local velocity fluctuations between consecutive collisions which appear very often at high packing fractions.

6. CONCLUSION

The comparison between experiments, numerical simulations, and kinetic theory is very close for the studies of 2D disklike particles moving randomly inside a square box. There is a good agreement between the self-diffusion coefficient derived from the air-table experiment and the one determined from a molecular dynamics model with hard-disk interactions. The decrease of the self-diffusion coefficient can be easily interpreted as the decrease of the granular temperature with increase in concentration according to the kinetic theory. The conservation of energy in the latter case is analogous to the balance between the loss of energy due to dissipative interparticle collisions and gain in the particle kinetic energy due to air flow fluctuations occurring in the air table.

ACKNOWLEDGMENTS

We are indebted to M. C. Alleno, I. Ippolito, J. W. Vallance, and J. Lemaitre for their helpful discussions and criticisms of this work. This research work was partially supported by a NATO International Collaborative Research Grant.

REFERENCES

1. J. Lemaitre, A. Gervois, H. Peerhossaini, D. Bideau, and J. P. Troadec, *J. Phys. D* **23**:1396 (1990).
2. E. J. Hinch and J. Lemaitre, *J. Fluid Mech.* **273**:313 (1994).
3. S. B. Savage and D. J. Jeffrey, *J. Fluid Mech.* **110**:225 (1981).
4. J. Lemaitre, J. P. Troadec, A. Gervois, and D. Bideau, *Europhys. Lett.* **14**(1):77 (1991).
5. D. Bideau, A. Gervois, L. Oger, and J. P. Troadec, *J. Phys. (Paris)* **47**:1697 (1986).
6. A. Einstein, *Investigations on the Theory of the Brownian Motion* (Dover, New York, 1956).
7. C. K. K. Lun, S. B. Savage, D. J. Jeffrey, and N. Chepurniy, *J. Fluid Mech.* **140**:223 (1984).
8. S. B. Savage, in *Physics of Granular Media*, D. Bideau and J. A. Dodds, eds. (Nova Science, 1992), p. 343.
9. S. B. Savage and R. Dai, *Mech. Materials* **16**:225 (1993).